Advance Sustainable Science, Engineering and Technology (ASSET)
Vol. 7, No.1, January 2025, pp. 0250111-01 ~ 0250111-011
ISSN: 2715-4211 DOI: https://doi.org/10.26877/asset.v7i1.1128

Optimizing Image Preprocessing for AI-Driven Cervical Cancer Diagnosis

Chandra Prasetyo Utomo[1,*], Neng Suhaeni[1], Nashuha Insani[1], Elan Suherlan[1], Nunung Ainur Rahmah[2], Ahmad Rusdan Utomo[2], Indra Kusuma[2], Muhamad Fathurachman[1], Dewa Nyoman Murti Adyaksa[3]

[1]Department of Informatics, Universitas YARSI, Jakarta 10510, Indonesia

[2]Faculty of Medicine, Universitas YARSI, Jakarta 10510, Indonesia

[3]Department of Anatomical Pathology, Universitas Gadjah Mada, Yogyakarta 55281, Indonesia

*chandra.prasetyo@yarsi.ac.id

Abstract. Cervical cancer ranks among the top causes of cancer-related deaths in women globally. Early detection is vital for improving patient survival rates. The multiclass classification of cervical cell images presents challenges primarily due to the notable variations in cell sizes across different classes. Conventional AI methods for diagnosing cervical cancer often rely on image-resizing techniques that overlook crucial features like relative cell dimensions, which impairs the models' ability to distinguish between classes effectively. This paper presents a novel AI-driven approach that employs constant padding to maintain the natural size differences among cells. Our method utilizes deep learning for both feature extraction and multiclass classification. We assessed the method using the publicly accessible SIPaKMeD dataset. Experimental findings indicate that our approach surpasses traditional image-resizing methods, especially in classes that are more challenging to predict. This strategy highlights AI's potential to improve cervical cancer diagnosis, offering a more precise and dependable tool for early detection. A reliable and precise AI model for diagnosing cervical cancer is crucial for promoting widespread screening and ensuring timely and effective treatment, which can ultimately lower mortality rates. By aiding early and accurate diagnosis, this approach aligns with global health efforts to alleviate the burden of cancer and other diseases, especially in areas with limited access to advanced healthcare services facilities.

Keywords: Artificial Intelligence, Cervical Cancer Diagnosis, Deep Learning, Medical Image Processing, and Pretrained Models

(Received 2024-10-15, Accepted 2024-12-31, Available Online by 2025-01-06)

1. Introduction

According to Global Cancer Statistics, approximately 604,000 new cases and 342,000 deaths from cervical cancer were reported in 2020 [1]. The highly effective primary (HPV vaccine) and secondary (screening) prevention measures made cervical cancer nearly wholly preventable. However, only 40% of women in low-income and middle-income countries (LMICs) have ever been screened for cervical cancer [2]. The standard liquid-based or Pap smear cytology is the most widely used diagnostic test for the early detection and prevention of cervical cancer. However, manually testing samples' tedious nature and complexity make them inaccessible in LMICs, including Indonesia [3]. Numerous studies have highlighted the substantial potential of machine learning (ML) and deep learning (DL) algorithms for disease prediction and treatment outcomes across diverse clinical contexts [4]. To fully integrate ML and DL into healthcare, advancements in data handling and model development are essential to effectively address the complexity of medical data and enhance predictive accuracy [5].

The primary objective of this research is to develop an AI-driven method for accurately diagnosing cervical cancer using image-based analysis. By focusing on the multiclass classification of cervical cell images, the study addresses the complexities of distinguishing between cancerous and pre-cancerous cell types. Our method seeks to maintain critical image features, such as cell size, often lost in conventional preprocessing steps, ultimately improving diagnostic accuracy across all classes.

One of the significant challenges in developing AI models for cervical cancer diagnosis is the difficulty of multiclass classification. Different classes of cervical cells, such as normal, pre-cancerous, and cancerous, exhibit varying sizes and morphologies. Some classes are inherently more challenging to predict than others due to overlapping features and subtle differences in cell structures. Traditional image preprocessing methods, such as resizing all images to a fixed dimension (e.g., 224 x 224 pixels), can result in the loss of critical information—particularly cell size, which is a distinguishing feature among classes. This limitation affects the model's ability to differentiate between certain classes.

Several studies have explored AI-based cervical cancer screening using Whole Slide Images (WSI). The Artificial Intelligence Cervical Cancer Screening System (AICCS) processed WSI by dividing them into small patches for patch-level detection based on TBS 2014 criteria, utilizing RetinaNet for detecting abnormalities [6][7]. YOLOv3 was integrated with Darknet-53 for detection and InceptionV3 for classification [8]. A patch-to-sample (P2S) method combined patch-level detection and transformer networks for more accurate diagnosis [9]. Faster R-CNN was employed to detect cervical cancer in 16,000 ThinPrep cytology test images across multiple hospitals, demonstrating practical model training using 1,407 image patches [10]. Despite significant advancements in cervical cancer screening using WSIs, challenges remain in improving accuracy and addressing label noise in large datasets.

Various approaches have been explored to enhance cervical cancer diagnosis using deep learning models. DeepCervix employed VGG16, VGG19, XceptionNet, and ResNet50 for feature extraction [11]. An enhanced Faster R-CNN model with a generative adversarial network (GAN) to improve shallow feature extraction, outperforming other models but still facing issues with noise and overlapping cells [12]. A GSConv and Grad-CAM model increased mAP by 1.9% and reduced computational costs on a TCT dataset but may struggle with overfitting in dense backgrounds [13]. Additional research includes applying YOLOv5 and Faster R-CNN, with YOLOv5 achieving 83% average precision for binary classification on the CRIC dataset [14], and a segmentation method with feature selection showing up to 98.88% accuracy on cancer detection [15]. Despite these advancements, gaps remain in handling noisy data and multi-class classification.

Numerous preprocessing techniques have been applied to enhance cervical cell classification. One approach used data augmentation methods like cropping, flipping, rotation, and scaling to improve model generalization [16]. Padding schemes, such as those employed with radiographs [17] and CNNs like InceptionV3 and AlexNet, have been shown to improve classification accuracy by retaining critical spatial information [18] [19]. Techniques such as zero-padding and normalization, combined with random transformations like shifts and rotations, were used to maintain the cell structure while

increasing data variability [20]. Despite these advancements, the challenge remains in improving classification accuracy for specific cell types and enhancing model robustness in diverse datasets.

While current methods for cervical cancer diagnosis using AI have shown promising results, they largely overlook the importance of preserving cell size information during image preprocessing. This gap is particularly evident in multiclass classification, where the inability to maintain the natural size ratios of cells diminishes the model's capacity to distinguish between certain cell types. Preprocessing techniques that retain these size features while ensuring that the model can effectively handle images of varying dimensions are needed.

To address this issue, we propose a novel approach that involves padding images. Specifically, all images are transformed to a uniform size of 600 x 600 pixels using constant padding, which preserves the relative size of cervical cells between classes. This approach ensures the model can leverage the natural size differences between classes as a critical feature during classification. By maintaining the original aspect ratios of the cells, we improve the model's ability to distinguish between different cell types. We validate the effectiveness of this method using the publicly available SIPaKMeD dataset [21], showing that constant padding outperforms conventional resizing in classification accuracy.

Our proposed method was evaluated on the SIPaKMeD dataset, which consists of cervical cell images across multiple classes. We compared the performance of our constant padding approach with traditional resizing techniques, using metrics such as accuracy, precision, recall, and F1-score. The experimental results demonstrate that our method preserves cell size information, improving classification performance, particularly in the more challenging classes.

This paper makes several key contributions to AI-based cervical cancer diagnosis. First, we introduce a new preprocessing method, constant padding, that preserves cell size information, which is crucial for effective multiclass classification. Second, we demonstrate the superiority of this approach over traditional resizing methods, particularly in distinguishing between classes that exhibit significant differences in cell size. Lastly, we validate our method using the SIPaKMeD dataset, providing a comprehensive evaluation that shows improved diagnostic accuracy and robustness. Our method promotes sustainable development in healthcare through innovative technologies that can be scaled and adapted to various medical applications aligned with the United Nations Sustainable Development Goal 3 (Good Health and Well-being) by improving access to accurate and early cervical cancer screenings, especially in low-resource settings.

The remainder of this paper is organized as follows: Section 2 reviews the existing literature on AI-based cervical cancer diagnosis and medical image analysis. Section 3 describes the proposed method, including constant padding and the model architecture. Section 4 presents the evaluation results, comparing the proposed method with traditional resizing approaches. Finally, Section 5 concludes the paper with a summary of findings and directions for future research.

2. Methods

2.1 Overall Framework

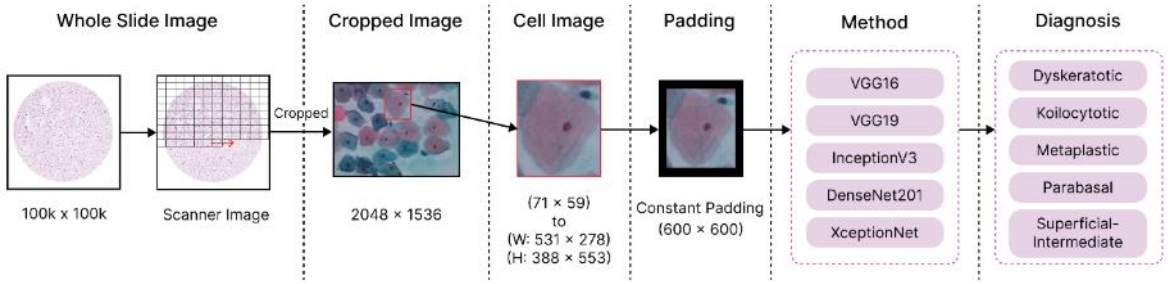

Figure 1. Proposed Methods

Figure 1 illustrates the proposed evaluation flow. Whole Slide images (WSI) from the SIPaKMeD dataset were manually cropped. The process generated 4,049 isolated cell images and 996 cluster cell images. The input we used includes isolated cell images with dimensions ranging from (71×59) to the largest size, which is 531×278 pixels (width) and 388×553 pixels (height).

To ensure that all images are of a consistent size, we apply a padding technique. The padding process starts by determining the desired final image size of 600 × 600 pixels. For each image, the amount of padding required on each side (top, bottom, left, and right) is calculated to position the image in the center of the added padding area. Padding is done by adding a black border around the image using the constant method, which allows the smaller image to fit the desired size without changing its proportions.

The approach was chosen to address the inherent differences in the sizes and morphologies of various classes of cervical cells. Accurately capturing these distinctions is critical for the model to differentiate between normal, pre-cancerous, and cancerous cells effectively. Traditional resizing methods often distort or lose these subtle yet significant details, negatively impacting classification accuracy. Conversely, constant padding preserves the original size information and ensures consistency across all classes, making it a robust preprocessing technique for this application.

In this experiment, we use pre-trained Convolutional Neural Networks (CNN) such as VGG-16, VGG-19, InceptionV3, DenseNet201, and XceptionNet to train our model with the padded data. The enhanced images were fed into the model for training, evaluation, and testing stages, allowing us to evaluate the model's performance in this classification task.

2.2 Data Preprocessing

Cells in the SIPaKMeD dataset vary in size due to differences in shape characteristics such as area, major and minor axis length, eccentricity, orientation, equivalent diameter, solidity, and area, as in Figure 2. These differences in each cell's nucleus and cytoplasm regions are essential for accurate analysis. Improper image preprocessing methods can adversely affect the model's performance, so choosing the proper preprocessing technique is critical.

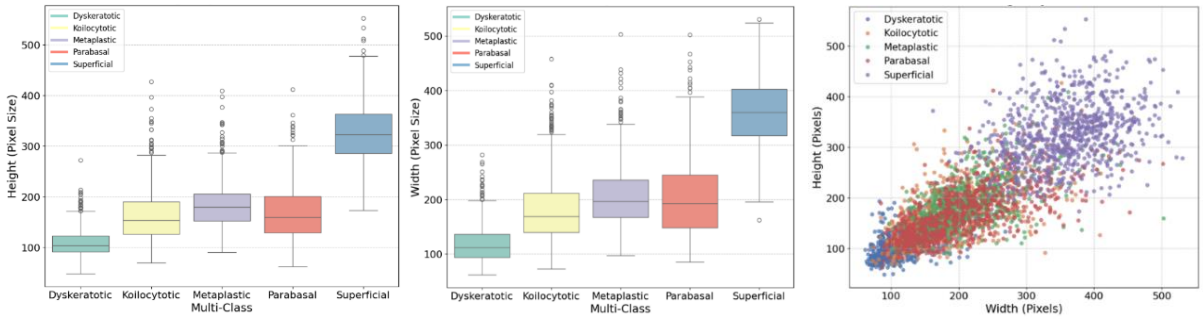

Figure 2. Image size distribution for each class (a) height distribution (b) width distribution (c) scatter plot of all images based on height and width

Adjusting each cell to a precise size, like 224×224 pixels, may lead to distortion and the risk of losing significant information, such as details about cell shape and structure. These distortions can impair the retention of crucial features necessary for accurate classification or detection. Thus, it is vital to employ preprocessing techniques that preserve the integrity of the original data.

Our study addressed this issue using the padding preprocessing technique. Padding involves adding borders around the image to achieve the desired input dimensions while maintaining the original aspect ratio. This method prevents distortion and preserves the data distribution of the cells. By applying

padding, we protect the cells' essential features, improving the model's ability to analyze and classify images accurately. The specific padding scheme used in our study is illustrated in Figure 3.

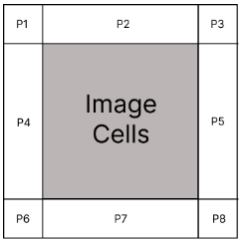

Figure 3. Constant Padding: Filled the padding area with (0, 0, 0)

2.3 Image Classifier

The study used several pre-trained CNN models to enhance the learning process: VGG16, VGG19, InceptionV3, DenseNet201, and Xception. For the VGG16 model, we employed the architecture pre-trained on the ImageNet dataset and modified the output of the "block4_conv3" layer. Additional layers, including GlobalMaxPooling2D, BatchNormalization, Dropout, and a Dense layer, were appended to enable classification into five categories. Similarly, for the VGG19 model, we used the ImageNet-pretrained architecture and froze all layers except for the last ten. The model was further enhanced with GlobalAveragePooling2D, BatchNormalization, Dropout, and a Dense layer for classification into five classes.

For the InceptionV3 model, we utilized the ImageNet-pretrained weights and froze all layers. The "mixed7" layer output was modified by adding GlobalMaxPooling2D, BatchNormalization, Dropout, and a Dense layer, facilitating five-class classification. In the case of the DenseNet201 model, the ImageNet-pretrained architecture was adopted, and all layers except the last ten were frozen to allow fine-tuning. The output from the "conv5_block16_concat" layer was modified with additional GlobalMaxPooling2D, BatchNormalization, and Dropout layers (using a rate of 0.4), along with a Dense layer sized at 2048 units for classification into five classes.

Lastly, the Xception model was employed with weights pre-trained on ImageNet, where all layers were frozen. We modified the "block14_sepconv1_act" output by incorporating GlobalAveragePooling2D, BatchNormalization, and Dropout layers (with a rate of 0.4). Additionally, two Dense layers with 1024 and 512 units, respectively, were added to facilitate five-class classification. This systematic approach to leveraging pre-trained architectures ensured optimized performance across the classification tasks.

3. Results and Discussion

This section comprehensively evaluates our proposed approach through experiments conducted on publicly available datasets. Specifically, we employ the SIPaKMeD dataset to assess the efficacy of our method in classifying cervical cell images into distinct categories. The details of the experimental setup, data distribution, and performance measures are provided below.

3.1 Experimental Data

We conducted experiments on the SIPaKMeD database [21]. The SIPaKMed database comprises 4,049 annotated images manually cropped from 966 cluster cell images into five categories by expert cytopathologists. Five main categories: (1) Dyskeratotic, (2) Koilocytotic, (3) Metaplastic, (4) Parabasal, and (5) Superficial-Intermediate are shown in Figure 4. Classes (1) Dyskeratotic and (2) Koilocytotic represent abnormal cervical cells, (4) Parabasal and (5) Superficial-Intermediate classes indicate normal cervical cells, and (3) Metaplastic represents benign cells. Categorized these classes are displayed in Table 1. The images were taken using a CCD camera (Infinity 1 Lumenera) attached to an

OLYMPUS BX53F optical microscope [26]. This database is suitable for classifying images and evaluating image segmentation techniques, whether they involve isolated cells (cropped images) or overlapping cells (cell cluster images). It includes each image's actual regions of interest as it contains ground truth. The properties of the SIPaKMeD database are shown in Table 2.

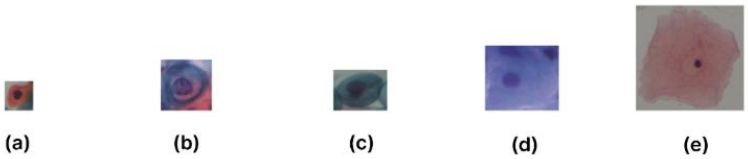

Figure 4. Original images from the SIPaKMeD: (a) Dyskeratotic, (b) Koilocytotic, (c) Metaplastic, (d) Parabasal, (e) Superficial-Intermediate

Table 1. The data distribution from the SIPaKMeD

Dataset	Category	Class	Number of Images	Number of cells
SIPaKMeD	Abnormal	Dyskeratotic	223	813
		Koilocytotic	238	825
	Benign	Metaplastic	271	793
	Normal	Parabasal	108	787
		Superficial-Intermediate	126	831
Total			966	4,049

Table 2. Detail properties SIPaKMeD databases

Property	SIPaKMeD
Data type	Image
Cells per image	Variable
Image Size	2,048 x 1,536 (pixel)
Format	.bmp
Number of images	966
Data Acquisition	Pap-smear
Classification	Manual
Class	5
Classified cells	4,049
Validation	Expert Cytopathologists
Download Page	https://www.cs.uoi.gr/~marina/sipakmed.html

3.2 Experimental Design

We employed the SIPaKMeD dataset, divided into 70% for training, 15% for validation, and 15% for testing in each class using a random_state setting with a value of 42 to ensure consistent data-sharing results each time the code is run. The resulting datasets are shown in Table 3. After dividing the data, we performed different preprocessing, namely resizing and padding. We applied several data augmentation techniques for the resizing method, including rescaling, shearing, zooming, and flipping the images. On the other hand, we directly preprocessed the data using constant padding for the padding method, ensuring that all images maintained uniform dimensions without altering the original aspect ratio. The example resizing data is in Figure 5, and padding is in Figure 6.

Table 3. The experimental data from the SIPaKMeD

Class	Training	Validation	Testing
Dyskeratotic	569	122	122
Koilocytotic	577	124	124
Metaplastic	555	119	119
Parabasal	550	118	119
Superficial-Intermediate	581	125	125
Total	2,832	608	609

Figure 5. Resize (224x224) from five categories of the SIPaKMeD dataset: (a)Dyskeratotic, (b)Koilocytotic, (c)Metaplastic, (d)Parabasal, (e)Superficial-Intermediate

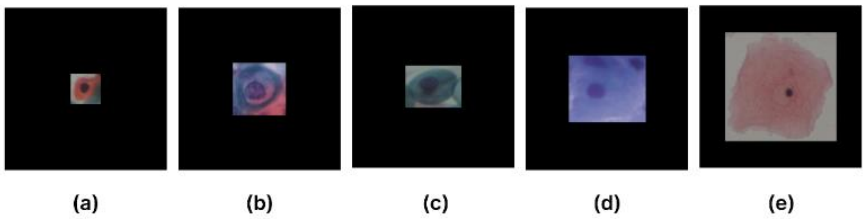

Figure 6. Constant Padding (600x600) from five categories of the SIPaKMeD dataset: (a)Dyskeratotic, (b)Koilocytotic, (c)Metaplastic, (d)Parabasal, (e)Superficial-Intermediate

We compared resizing and padding using five methods to evaluate accuracy and other metrics. One critical stage in developing and implementing a machine learning model is evaluation, which measures how well the model can predict or classify new data. Evaluation metrics vary depending on the problem type. For classification problems, accuracy, precision, recall, and F1-score are standard measures to evaluate classification performance [27]. Our experiment's quality was measured using these metrics, calculated based on true positive (TP), true negative (TN), false positive (FP), and false negative (FN) values.

$$Accuracy = \frac{TP+TN}{TP+TN+FP+FN} \quad (1)$$

$$Precision = \frac{TP}{TP+FP} \quad (2)$$

$$Recall = \frac{TP}{TP+FN} \quad (3)$$

$$F1Score = 2\frac{Precision.Recall}{Precision+Recall} \quad (4)$$

The model is trained for 50 epochs using a GPU NVIDIA GeForce RTX 4090 with 24 GB dedicated memory and 64 GB RAM. During training, we employed Adam as the optimizer. The initial learning rate is set to 0.0001, and the loss function is calculated using categorical cross-entropy. We apply the early stopping method in the validation stage. The training process will only be stopped if the model's accuracy improves within 10 consecutive iterations. The code for this implementation is publicly available at https://github.com/YARSIAICenter/cervical_cancer_padding/.

3.3 Result and Analysis

We compared our proposed method (padding) with standard image preprocessing (resize) using five popular pre-trained models: VGG16, VGG19, InceptionV3, DenseNet201, and Xception. Our experiments revealed notable differences in performance between the two methods, which we assessed using accuracy, precision, recall, and F1-score. We calculated macro averages for precision, recall, and F1-score to ensure a balanced evaluation across all classes. This approach treats each class equally, regardless of its size or frequency, making it particularly valuable for multiclass classification tasks where fairness across all classes is essential. The evaluation results are presented in Table 4. Our proposed method outperformed the baseline method in all metrics. DenseNet201 is the classifier with the highest performance with an accuracy of 0.9524, precision of 0.9522, recall of 0.9526, and F1-score of 0.9521.

Table 4. Comparison of Resize vs. Padding performance

Preprocessing	Method	Classes	Accuracy	Precision	Recall	F1-Score
Resize	VGG16	5	0.8539	0.8530	0.8538	0.8518
	VGG19	5	0.8489	0.8633	0.8494	0.8478
	InceptionV3	5	0.8916	0.8903	0.8918	0.8908
	DenseNet201	5	0.9458	0.9456	0.9462	0.9457
	Xception	5	0.9212	0.9202	0.9212	0.9204
Padding	VGG16	5	0.8719	0.8731	0.8721	0.8701
(Proposed Method)	VGG19	5	0.8834	0.8908	0.8823	0.8822
	InceptionV3	5	0.9031	0.9025	0.9031	0.9026
	DenseNet201	**5**	**0.9524**	**0.9522**	**0.9526**	**0.9521**
	Xception	5	0.9392	0.9389	0.9392	0.9390

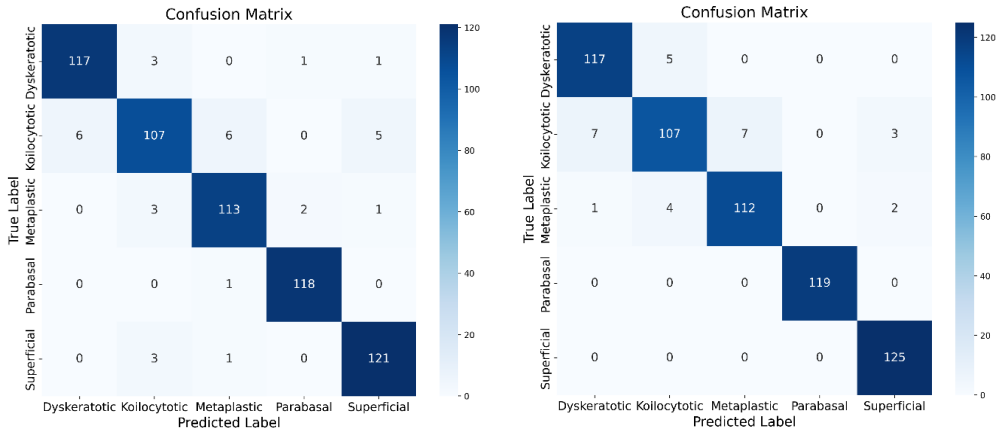

(a) (b)

Figure 7. Confusion Matrix: (a) DenseNet201 (Resize), (b) DenseNet201 (Padding)

We analyze the performance of the best model in our proposed method, DenseNet201, through a comparative analysis of two preprocessing techniques: resizing and padding. The Confusion Matrix, presented in Figure 7, highlights the model's performance in classifying dyskeratotic, koilocytotic, metaplastic, parabasal, and superficial cells. Both preprocessing methods yield consistent results in classifying dyskeratotic cells, with each approach correctly identifying 117 samples. This consistency suggests that the model effectively captures the distinctive features of dyskeratotic cells, regardless of the preprocessing technique used. However, the classification of koilocytotic cells showed moderate

misclassifications in both methods. Specifically, the resizing approach misclassified 6 samples as metaplastic, 6 as dyskeratotic, and 5 as superficial, while the padding method misclassified 7 samples as dyskeratotic, 7 as metaplastic, and 3 as superficial. These misclassifications indicate that koilocytotic cells share overlapping features with other cell types, complicating their accurate classification. In the case of metaplastic cells, the resizing method slightly outperformed the padding method, correctly classifying 113 samples compared to 112.

The padding method performed better for parabasal cells, correctly classifying 119 samples. This is likely due to padding's ability to preserve the original aspect ratio and contextual information. The most notable improvement was observed in classifying superficial cells, where the padding method correctly identified 125 samples compared to 121 under the resizing approach. This result underscores the advantage of padding in retaining critical morphological details, particularly for this class.

Following the technical analysis of the performance across different classes, we considered analyzing the biological insights behind the varying results observed in our models. Implementing constant padding as a preprocessing technique has demonstrated significant advantages over traditional resizing methods, particularly in preserving critical image features biologically relevant for accurate cervical cancer diagnosis. Traditional resizing often distorts important spatial information, especially the relative size differences between cells, essential for distinguishing between normal, pre-cancerous, and cancerous cells [28].

Different cervical cell types exhibit distinct sizes and morphologies, vital indicators of their health status. Constant padding preserves these size differences by maintaining the original aspect ratios and sizes of the cells, allowing the model to differentiate between cell types more effectively. This ability to retain natural size variations enhances diagnostic accuracy by aligning with the biological characteristics observed in cervical cancer.

Constant padding addresses a significant gap in AI-based methods by preserving spatial relationships within the images. As seen in our experimental results, this improves performance in classifying cells based on their morphological features. In conclusion, padding generally enhances model performance in specific classes by maintaining object structure, while resizing is more effective for classes with intricate details. Therefore, the choice of preprocessing method should be tailored to the specific characteristics of the image data and the target classes for optimal results.

4. Conclusion

In this paper, we present an AI-driven method for cervical cancer diagnosis that addresses the challenges of multiclass classification, specifically the loss of cell size information in conventional preprocessing techniques. By using constant padding to preserve the natural size ratios of cervical cells, our approach demonstrated improved classification accuracy, especially in the more difficult-to-predict classes. Evaluation of the SIPaKMeD dataset confirmed that preserving this feature leads to superior performance compared to traditional resizing methods.

Our results suggest that incorporating size-preserving techniques in image preprocessing is crucial for improving the accuracy and robustness of AI models in cervical cancer diagnosis. By supporting early and accurate diagnosis, this method aligns with global health initiatives aimed at reducing the burden of cancer and other diseases, particularly in regions with limited access to advanced healthcare facilities. Policymakers can leverage these findings to advocate for increased investment in AI technology and training for healthcare professionals, ensuring that the benefits of such advancements are accessible to a broader population.

One limitation is the reliance on the SIPAKMED dataset, which may not fully represent the diversity of cervical cell images encountered in different populations. Future studies should evaluate the method on a more diverse data set to ensure its generalizability across various demographic and geographic contexts. Additionally, further research is needed to integrate this method with other diagnostic tools and technologies (multimodal approaches), such as molecular testing and electronic

health records, to create a more comprehensive diagnostic system. It will also be crucial to investigate the scalability of this approach in real-world clinical settings and its impact on workflow efficiency and patient outcomes. Overall, this study lays the groundwork for more accurate and reliable AI-based diagnostic methods, which have the potential to significantly advance the field of medical imaging and improve healthcare delivery.

Acknowledgments

This research is partially funded by Matching Fund Kedaireka from the Ministry of Education and Research, Republic of Indonesia, and by Internal Research Grant Universitas YARSI 2024, with Grant ID 192/WR II/PN.00/V/2024.

References

[1] H. Sung *et al.*, "Global Cancer Statistics 2020: GLOBOCAN Estimates of Incidence and Mortality Worldwide for 36 Cancers in 185 Countries," *CA. Cancer J. Clin.*, vol. 71, no. 3, pp. 209–249, 2021, doi: 10.3322/caac.21660.

[2] J. M. Lemp *et al.*, "Lifetime Prevalence of Cervical Cancer Screening in 55 Low-and Middle-Income Countries," *JAMA - J. Am. Med. Assoc.*, vol. 324, no. 15, pp. 1532–1542, 2020, doi: 10.1001/jama.2020.16244.

[3] D. Saslow *et al.*, "American Cancer Society, American Society for Colposcopy and Cervical Pathology, and American Society for Clinical Pathology screening guidelines for the prevention and early detection of cervical cancer," *CA. Cancer J. Clin.*, vol. 62, no. 3, pp. 147–172, May 2012, doi: 10.3322/CAAC.21139.

[4] M. K. Maysaa R. Naeemah, "Advances in Deep Learning for Skin Cancer Diagnosis", doi: https://doi.org/10.26877/asset.v6i4.1002.

[5] Abdillah, S. Syaharuddin, V. Mandailina, and S. Mehmood, "The Role of Mathematics in Machine Learning for Disease Prediction: An In-Depth Review in the Healthcare Domain," *Adv. Sustain. Sci. Eng. Technol.*, vol. 6, no. 4, p. 02404010, 2024, doi: 10.26877/asset.v6i4.845.

[6] J. Wang *et al.*, "Artificial intelligence enables precision diagnosis of cervical cytology grades and cervical cancer," *Nat. Commun.*, vol. 15, no. 1, pp. 1–14, 2024, doi: 10.1038/s41467-024-48705-3.

[7] X. Zhu *et al.*, "Hybrid AI-assistive diagnostic model permits rapid TBS classification of cervical liquid-based thin-layer cell smears," *Nat. Commun.*, vol. 12, no. 1, pp. 1–12, 2021, doi: 10.1038/s41467-021-23913-3.

[8] Y. Xiang, W. Sun, C. Pan, M. Yan, Z. Yin, and Y. Liang, "A novel automation-assisted cervical cancer reading method based on convolutional neural network," *Biocybern. Biomed. Eng.*, vol. 40, no. 2, pp. 611–623, 2020, doi: 10.1016/j.bbe.2020.01.016.

[9] M. Cao *et al.*, "Patch-to-Sample Reasoning for Cervical Cancer Screening of Whole Slide Image," *IEEE Trans. Artif. Intell.*, vol. PP, pp. 1–11, 2023, doi: 10.1109/TAI.2023.3323637.

[10] X. Tan *et al.*, "Automatic model for cervical cancer screening based on convolutional neural network: a retrospective, multicohort, multicenter study," *Cancer Cell Int.*, vol. 21, no. 1, pp. 1–10, 2021, doi: 10.1186/s12935-020-01742-6.

[11] M. M. Rahaman *et al.*, "DeepCervix: A deep learning-based framework for the classification of cervical cells using hybrid deep feature fusion techniques," *Comput. Biol. Med.*, vol. 136, no. May, p. 104649, 2021, doi: 10.1016/j.compbiomed.2021.104649.

[12] L. Xu, F. Cai, Y. Fu, and Q. Liu, "Cervical cell classification with deep-learning algorithms," *Medical and Biological Engineering and Computing*, vol. 61, no. 3. pp. 821–833, 2023. doi: 10.1007/s11517-022-02745-3.

[13] Y. Guo, D. Chen, C. Bao, and Y. Luo, "Causal Attention-Based Lightweight and Efficient Cervical Cancer Cell Detection Model," *2023 IEEE Int. Conf. Bioinforma. Biomed.*, pp. 1104–1111, 2023, doi: 10.1109/BIBM58861.2023.10385353.

[14] M. Kalbhor, S. Shinde, P. Wajire, and H. Jude, "CerviCell-detector: An object detection approach for identifying the cancerous cells in pap smear images of cervical cancer," *Heliyon*, vol. 9, no. 11, p. e22324, 2023, doi: 10.1016/j.heliyon.2023.e22324.

[15] W. William, A. Ware, A. H. Basaza-Ejiri, and J. Obungoloch, "A pap-smear analysis tool (PAT) for detection of cervical cancer from pap-smear images," *Biomed. Eng. Online*, vol. 18, no. 1, pp. 1–22, 2019, doi: 10.1186/s12938-019-0634-5.

[16] I. Pacal and S. Kılıcarslan, "Deep learning-based approaches for robust classification of cervical cancer," *Neural Comput. Appl.*, vol. 35, no. 25, pp. 18813–18828, 2023, doi: 10.1007/s00521-023-08757-w.

[17] M. Model and S. Liang, "Towards Robust and Accurate Detection of Abnormalities in Musculoskeletal Radiographs with", doi: 10.3390/s20113153.

[18] H. Tang, A. Ortis, and S. Battiato, *The impact of padding on image classification by using pre-trained convolutional neural networks*, vol. 11752 LNCS. Springer International Publishing, 2019. doi: 10.1007/978-3-030-30645-8_31.

[19] T. Haryanto, I. S. Sitanggang, M. A. Agmalaro, and R. Rulaningtyas, "The Utilization of Padding Scheme on Convolutional Neural Network for Cervical Cell Images Classification," *CENIM 2020 - Proceeding Int. Conf. Comput. Eng. Network, Intell. Multimed. 2020*, pp. 34–38, 2020, doi: 10.1109/CENIM51130.2020.9297895.

[20] T. Albuquerque, R. Cruz, and J. S. Cardoso, "Ordinal losses for classification of cervical cancer risk," *PeerJ Comput. Sci.*, vol. 7, pp. 1–21, 2021, doi: 10.7717/peerj-cs.457.

[21] SIPaKMeD, "SIPaKMeD Database." [Online]. Available: https://www.cs.uoi.gr/~marina/sipakmed.html

[22] K. Simonyan and A. Zisserman, "Very deep convolutional networks for large-scale image recognition," *3rd Int. Conf. Learn. Represent. ICLR 2015 - Conf. Track Proc.*, pp. 1–14, 2015.

[23] C. Szegedy, V. Vanhoucke, S. Ioffe, J. Shlens, and Z. Wojna, "Rethinking the Inception Architecture for Computer Vision," *Proc. IEEE Comput. Soc. Conf. Comput. Vis. Pattern Recognit.*, vol. 2016-Decem, pp. 2818–2826, 2016, doi: 10.1109/CVPR.2016.308.

[24] G. Huang, Z. Liu, L. Van Der Maaten, and K. Q. Weinberger, "Densely connected convolutional networks," *Proc. - 30th IEEE Conf. Comput. Vis. Pattern Recognition, CVPR 2017*, vol. 2017-Janua, pp. 2261–2269, 2017, doi: 10.1109/CVPR.2017.243.

[25] F. Chollet, "Xception: Deep learning with depthwise separable convolutions," *Proc. - 30th IEEE Conf. Comput. Vis. Pattern Recognition, CVPR 2017*, vol. 2017-Janua, pp. 1800–1807, 2017, doi: 10.1109/CVPR.2017.195.

[26] M. E. Plissiti, G. Sfikas, C. Nikou, and A. Charchanti, "Sipakmed : A New Dataset for Feature and Image Based Classification of Normal and Pathological Cervical Cells in Pap Smear Images SIPAKMED : A NEW DATASET FOR FEATURE AND IMAGE BASED CLASSIFICATION OF," no. October, 2018, doi: 10.1109/ICIP.2018.8451588.

[27] R. F. Ribeiro, H. R. Torres, B. Oliveira, and ..., "Deep Learning Methods for Lesion Detection on Full Screening Mammography: A Comparative Analysis," *3rd Symposium of …*. bibliotecadigital.ipb.pt, 2023.

[28] W. A. Mustafa, S. Ismail, F. S. Mokhtar, H. Alquran, and Y. Al-Issa, "Cervical Cancer Detection Techniques: A Chronological Review," *Diagnostics*, vol. 13, no. 10, 2023, doi: 10.3390/diagnostics13101763.